JOURNAL OF SPACECRAFT AND ROCKETS
Vol. 29, No. 2, March–April 1992

Constant Reverse Thrust Activated Reorientation of Liquid Hydrogen with Geyser Initiation

R. J. Hung* and K. L. Shyu†
University of Alabama in Huntsville, Huntsville, Alabama 35899

A key objective of the cryogenic fluid management of the spacecraft propulsion system is to develop the technology necessary for acquisition or positioning of liquid outflow or vapor venting. In this paper, numerical simulation of positive liquid acquisition is attempted by introducing reverse gravity acceleration, resulting from the propulsive thrust of auxiliary engines, which exceeds critical value for the initiation of geyser. Based on the computer simulation of flowfields during the course of fluid reorientation, six dimensionless parameters resulted in this study. It shows that these parameters hold near-constant values through the entire ranges of liquid filled levels, from 30–80%, during the course of fluid reorientation.

Nomenclature

a_g = geyser initiation acceleration, cm/s^2
a_m = scale flow acceleration associated with maximum velocity (cm/s^2), defined by Eq. (5)
D = diameter of propellant tank, cm
f = frequency of impulsive thrust, Hz
g_i = geyser initiation gravity level, g_0
g_0 = normal Earth gravitational acceleration, 9.81 m/s^2
$\bar{h}$ = average liquid height, cm
h_m = maximum liquid height, cm
L = height of propellant tank, cm
L_m = scale length of maximum liquid height (cm), defined by Eq. (4)
$\bar{t}_f$ = average free-fall time, s
t_m = time for observing maximum flow velocity, s
t_R = liquid reaching tank bottom time, s
$\bar{V}_f$ = average free-fall velocity (cm/s), defined by Eq. (2)
V_{fm} = free-fall velocity from maximum liquid height (cm/s), defined by Eq. (3)
V_m = maximum flow velocity, cm/s

I. Introduction

HANDLING and control of cryogenic fluids in liquid propulsion systems become important in a low-gravity environment. In liquid-rocket-powered spacecraft in low Earth orbit or in transit to the lunar or Martian orbits, residual propellant can migrate away from the fuel tank drains (engine fuel lines), which would preclude the restarting of engines after a period of time at low gravity. Additional concern centered around the reorientation of liquid fuels before an engine is started and the liquid is subjected to acceleration for reorientation. The sloshing of liquid in a partially filled tank in low gravity constituted another problem. For the case of cryogenic liquids used as propellants, heat transfer from the surroundings can lead to evaporation. To design proper tank pressurization and venting systems, it is necessary to know where the liquid and the vapor are disturbed within the tank in low gravity.

A key objective of the cryogenic fluid management of spacecraft propulsion system, such as a Space Transfer Vehicle[1] (STV) and other space vehicles, is to develop the technology necessary for acquisition or positioning of liquid and vapor within a tank in reduced gravity to enable liquid outflow or vapor venting. Liquid acquisition techniques can be divided into two general categories: 1) active liquid acquisition by the creation of a positive acceleration environment resulting from the propulsive thrust of small auxiliary engines, and 2) passive liquid acquisition utilizing the liquid capillary forces provided by using solid baffles of liquid traps made of fine mesh screen material. In this study, active liquid acquisition is aimed for numerically simulating the resettlement of cryogenic liquid hydrogen. Liquid hydrogen (due to its low boiling point, low kinematic viscosity, low thermal conductivity, explosive, hazardous, etc.), which, in general, poses more severe technical challenges than liquid oxygen, is used as the test bed working fluid in this study.

Recently, Leslie[2] was able to measure and to numerically compute the bubble shapes at various ratios of centrifugal force to surface tension force in the microgravity environment. Hung and Leslie[3] extended Leslie's work[2] to rotating free surfaces influenced by gravity with higher rotating speeds when the bubble intersects with both the top and bottom walls of the cylinder. Hung et al.[4,5] further extended the work to include rotating speeds which resulted with bubbles intersecting and/or without intersecting the top, bottom, and side walls of the cylinder.

An analysis of time-dependent dynamical behavior of surface tension on partially filled rotating fluids in both low-gravity and microgravity environments was carried out by numerically solving the Navier-Stokes equations subjected to the initial and the boundary conditions.[4,6] The initial condition for the bubble profiles was adopted from steady-state formulations developed by Hung and Leslie[3] and Hung et al.[6] for rotating cylinder tank; and by Hung et al.[5,7] for the Dewar-shaped container to be used in the Gravity Probe-B Spacecraft.[8] Some of the steady-state formulations of bubble shapes, in particular for bubbles intersecting at the top wall of the cylinder, were compared with the experiment carried out by Leslie[2] in a free-falling aircraft (KC-135) with excellent agreement.

An efficient propellant settling technique should minimize propellant usage and weight penalties. This can be accomplished by providing optimal acceleration to the spacecraft such that the propellant is reoriented over the tank outlet without any vapor entrainment, any excessive geysering, or any other undesirable fluid motion.

Production of geyser during the propellant reorientation is not a desirable motion for the space fluid management. It is because geyser is always accompanied by the vapor entrainment and globule formation. Geyser is observed at reverse gravity acceleration greater than certain critical values of acceleration during the course of liquid reorientation. In other words, geyser will not be observed at a very low reverse gravity

Received June 14, 1990; revision received May 12, 1991; accepted for publication May 12, 1991.

*Professor. Associate Fellow AIAA.
†Staff Engineer.

level, and it will be detected when the reverse gravity level is greater than the certain critical level. In this paper, numerical simulation of positive liquid acquisition is attempted by introducing reverse gravity acceleration, resulting from the propulsive thrust of small auxiliary engines that exceeds the critical value for geyser initiation. The reverse gravity acceleration starts with a small value and increases gradually until the initiation of geyser is detected in the computer simulation for the liquid reorientation of propellant tank with various liquid-filled levels.

In this study, time-dependent computations of Navier-Stokes equations have been carried out to investigate the dynamical behavior of liquid reorientation with geyser initiation prior to main engine firing for spacecraft restart. The computation extends to the study of the characteristics of liquid resettlement due to the reversal of lowest artificial gravity fields with geyser initiation with and without imposing frequencies of impulsive acceleration. This frequency of impulsive acceleration is generally termed "gravity jitters." Gravity jitters are produced by spacecraft attitude motion, machinery (turbine, pump, engine) vibrations, thruster firing, thruster shutdown, etc.[9] Positioning of liquid propellant over the tank outlet can be carried out by using small auxiliary thrusters that provide a thrust parallel to the tank's major axis in the direction of flight.

II. Numerical Simulation of Liquid Hydrogen Reorientation at the Reverse Gravity Acceleration with Geyser Initiation

Propellant tank of liquid-filled levels of 30, 50, 65, 70, and 80% are considered in this study. Time-dependent axisymmetric mathematical formulation of Navier-Stokes equations are adopted. Detailed description of the mathematical formulation and initial and boundary conditions suitable for the analysis of cryogenic fluid management under microgravity environment are given in our earlier studies.[4,6,10-15] The initial profiles of liquid-vapor interface are determined from computations based on algorithms developed for the steady-state formulation of microgravity fluid management.[3-7]

A staggered grid for the velocity components is used in this computer program. The method was first developed by Harlow and Welch[16] for their MAC (marker and cell) method of studying fluid flows along free surface. The finite difference method employed in this numerical study was the "Hybrid Scheme" developed by Spalding.[17] The formulation for this method is valid for any arbitrary interface location between the grid points and is not limited to middle point interfaces.[18] An algorithm for semi-implicit method[19] was used as the procedure for modeling the flowfield. The time step is determined automatically based on the size of the grid points and the velocity of flowfields. Detailed descriptions of the computational algorithm applicable to microgravity fluid management are illustrated in our earlier studies.[4,6,10-15] Figure 1a shows the distribution of grid points in the radial-axial plane of axisymmetric cylindrical coordinates.

For the purpose of facilitating easy comparison between computational results and experimental measurement, a subscale model of 0.01 size prototype is adopted in the computer simulation. Figure 1b shows a model size for computation. The size of the prototype is height, $L = 423.672$ cm (166.8 in.), and diameter, $D = 426.72$ cm (168 in.). Subscale model size is $L = 4.23672$ cm and $D = 4.2672$ cm, as shown in Fig. 1b. If the spacecraft had been coasting for a long time, aligned with its direction of motion, the most significant force, drag, would be axial and with acceleration of 10^{-4} g_0 along the upward direction. The hydrogen vapor is, thus, originally positioned at the bottom (outlet side) of the tank. The requirement to settle or to position liquid fuel over the outlet end of the spacecraft propellant tank prior to main engine restart poses a microgravity fluid behavior problem.[10] Retromaneuvers of spacecraft, such as STV and other spacecraft, require settling or reorientation of the propellant prior to main engine firing.[1,10] Cryogenic liquid propellant shall be positioned over the tank outlet by using auxiliary thrusters (or idle-mode thrusters from the main engine) that provide a thrust parallel to the tank's major axis in the direction of flight. In the present study of computer simulation, a small value of reverse gravity acceleration (downward direction) is provided by the propulsive thrust of a small auxiliary engine to initiate the reorientation of liquid propellant. This small value of reverse gravity acceleration of propulsive thrust increases gradually until reaching the critical value on which the initiation of geyser is detected during the time period of fluid resettlement. We term this reverse gravity acceleration of propulsive thrust, which is capable to initiate geyser, as "geyser initiation gravity-level." This geyser initiation gravity level has been investigated through the method of trial and error for the various liquid-filled levels of propellant tank as a base to simulate the following cases of reduced gravity fluid behaviors during the reorientation: 1) constant reverse gravity acceleration, 2) impulsive reverse gravity acceleration with a frequency of 0.1 Hz, 3) impulsive reverse gravity acceleration with a frequency of 1.0 Hz, and 4) impulsive reverse gravity acceleration with a frequency of 10 Hz. Cases 2–4 for the impulsive reverse gravity acceleration with various frequencies will be discussed and published in the subsequent papers.[13,15,20] Liquid-filled levels of 30, 50, 65, 70, and 80% have been considered in this study. Cryogenic liquid hydrogen at a temperature of 20 K is considered. Liquid hydrogen density of 0.071 g/cm^3, surface tension coefficient at the interface between liquid hydrogen and hydrogen vapor of 1.9 dyne/cm, liquid hydrogen viscosity coefficient of 1.873×10^{-3} cm^2/s, and contact angle of 0.5 deg are used in the computer simulation.

Reorientation of cryogenic liquid hydrogen activated reverse gravity acceleration with geyser initiation has been investigated for various liquid-filled levels of propellant tank. It is found that these geyser initiation gravity levels are 5.5×10^{-2}, 6.52×10^{-2}, 6.6×10^{-2}, 6.7×10^{-2}, and 8.2×10^{-2} g_0 for

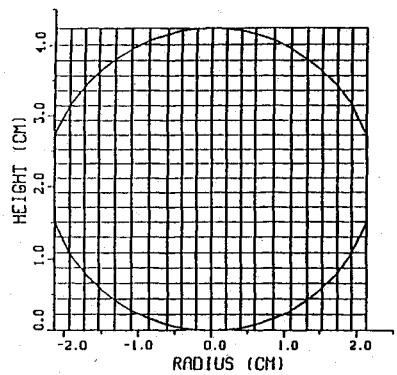

Fig. 1a Distribution of grid points in the radial-axial plane of cylindrical coordinate for propellant tank.

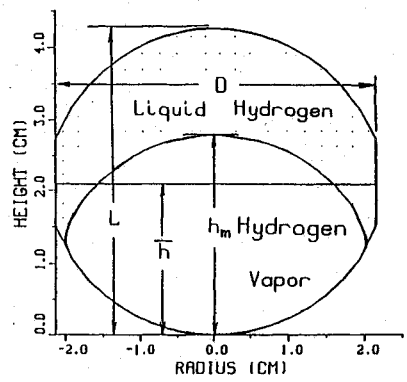

D-4.26720 CM, L-4.23672 CM

Fig. 1b Model size propellant tank adopted for numerical simulation with geometrical description.

Table 1 Characteristics of cryogenic hydrogen reorientation (frequency of impulsive acceleration = 0.0 Hz)

Liquid-filled level, %	30	50	65	70	80
Geyser initiation gravity-level g_i, $(10^{-2}g_0)$	5.5	6.52	6.6	6.7	8.2
Geyser initiation acceleration a_g, cm/s^2	53.9	63.9	64.7	65.7	80.4
Average liquid height $\bar{h}$, cm	2.67	2.05	1.52	1.35	0.93
Average free-fall flow velocity $\bar{V}_f$, cm/s	17.0	16.2	14.0	13.3	12.5
Maximum flow velocity V_m, cm/s	73.6	72.6	68.5	65.7	62.0
$V_m/\bar{V}_f$	4.3	4.5	4.8	4.9	4.9
Average free-fall time $\bar{t}_f$, s	0.32	0.25	0.22	0.20	0.15
Liquid reaching bottom time t_R, s	0.40	0.31	0.27	0.25	0.20
$t_R/\bar{t}_f$	1.25	1.21	1.25	1.25	1.30
Time for observing maximum flow velocity t_m, s	0.42	0.31	0.28	0.25	0.20
Scale length of maximum flow velocity L_m ($= V_m t_m$), cm	30.9	23.2	19.2	16.7	12.4
$L_m/\bar{h}$	11.6	11.6	12.4	12.3	13.0
$t_m/\bar{t}_f$	1.3	1.2	1.3	1.3	1.3
Scale flow acceleration associated with maximum velocity a_m ($= V_m/t_m$), cm/s^2	175	232	244	257	310
a_m/a_g	3.3	3.6	3.7	3.9	3.8
Maximum liquid height h_m, cm	3.41	2.79	2.26	2.09	1.67
Free-fall velocity from maximum liquid height V_{fm}, cm/s	19.2	18.9	17.1	16.6	16.4
V_m/V_{fm}	3.9	3.8	4.0	3.9	3.8

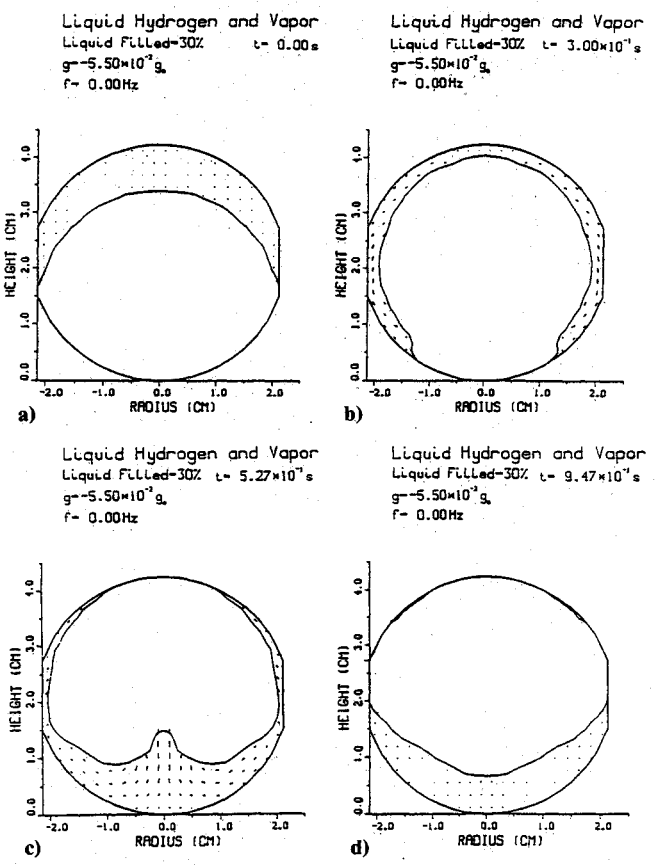

Fig. 2 Selected sequences of time evolution of fluid reorientation with liquid-filled level of 30%: a) initial profile; b) flow profile before the initiation of geyser; c) flow profile with geyser; and d) flow profile after the ending of geyser.

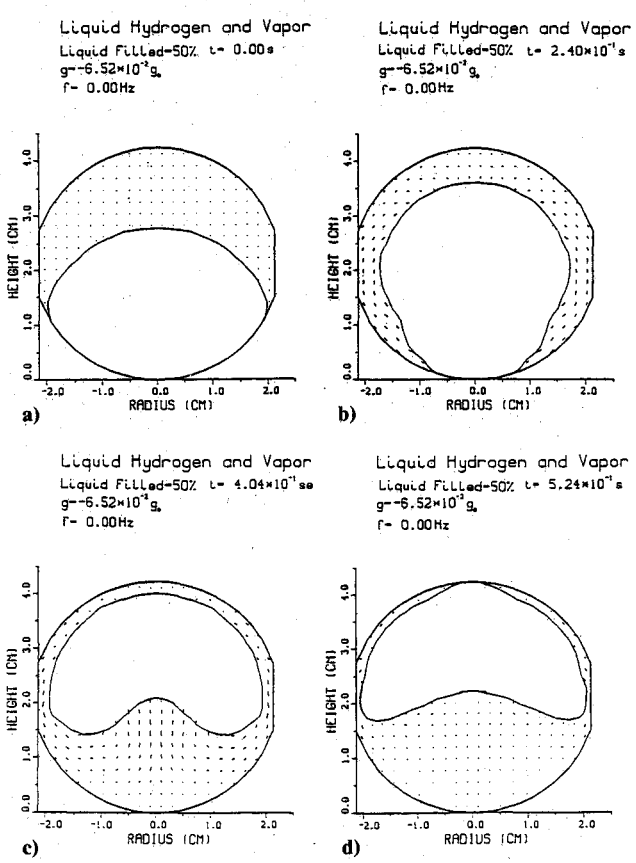

Fig. 3 Selected sequences of time evolution of fluid reorientation with liquid-filled level of 50%: a) initial profile; b) flow profile before the initiation of geyser; c) flow profile with geyser; and d) flow profile after the ending of geyser.

liquid-filled levels of 30, 50, 65, 70, and 80%, respectively (see Table 1 for listings). Figures 2–6 show the selected sequences of time evolution of fluid reorientation for cryogenic hydrogen with liquid-filled levels of 30, 50, 65, 70, and 80%, respectively. Detailed description of the variations in physical parameters in terms of liquid-filled levels are illustrated in Table 1. Each figure contains four subfigures. Subfigure a is the initial profile of liquid-vapor interface at the moment of the starting of fluid reorientation at time $t = 0$; subfigure b is the flow profile during the course of fluid reorientation before the initiation of geysering motion; subfigure c is the flow profile with geysering motion; and subfigure d is the flow profile after the ending of geysering motion.

Figures 2–6 also illustrate the following flow behaviors: 1) The liquid starts to flow in an annular sheet along the solid wall of tank and gradually pushes the vapor toward the central portion of the lower dome of the tank as the net acceleration, reversing the direction of gravity field, which is applied toward the downward direction of the tank's major axis, by using small auxiliary thrusters. 2) As the downward fluid

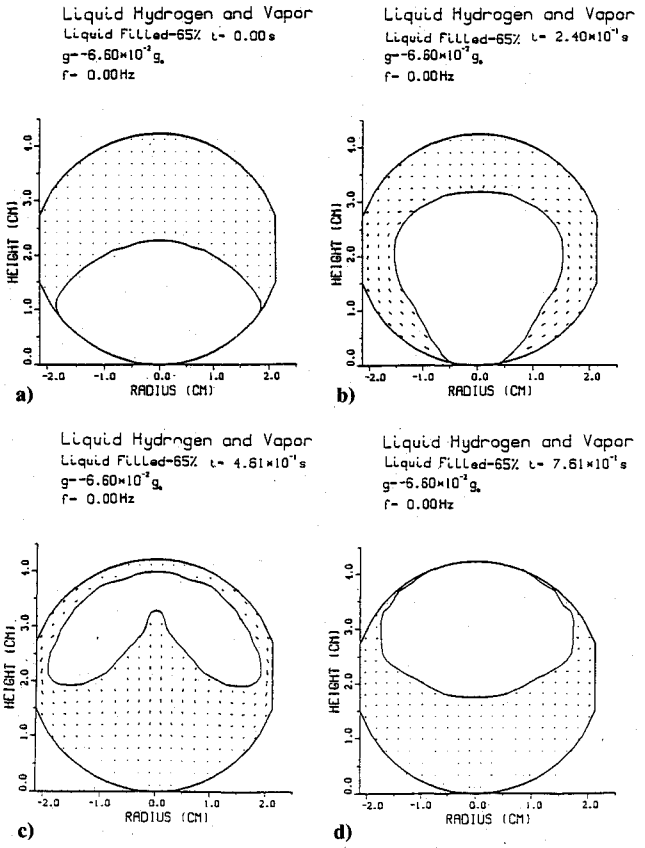

Fig. 4 Selected sequences of time evolution of fluid reorientation with liquid-filled level of 65%: a) initial profile; b) flow profile before the initiation of geyser; c) flow profile with geyser; and d) flow profile after the ending of geyser.

annular sheet along the tank wall reaches the central bottom dome side of the tank, a geysering flow is observed. 3) The vapor is thus pushed upward centrally into the liquid and the geysering disappears.

Furthermore, Table 1 shows the characteristics of cryogenic liquid hydrogen resettlement activated by reverse gravity acceleration with geyser initiation. Average liquid height $\bar{h}$ and maximum liquid height h_m are shown in Fig. 1b. Average free-fall velocity $\bar{V}_f$, average free-fall time $\bar{t}_f$, and free-fall velocity from maximum liquid height V_{fm} are computed from the following equations:

$$\bar{V}_f = (2g_i\bar{h})^{1/2} \tag{1}$$

$$\bar{t}_f = (2\bar{h}/g_i)^{1/2} \tag{2}$$

$$V_{fm} = (2g_i h_m)^{1/2} \tag{3}$$

where g_i denotes reverse gravity acceleration with geyser initiation. Values of maximum flow velocity V_m, time required for observing maximum flow velocity t_m, and time needed for reorienting liquid flowing down and reaching the bottom of propellant tank t_R are obtained from the numerical computation of flowfield. Scale length of maximum flow velocity L_m and scale flow acceleration associated with maximum flow velocity a_m are computed from the following parameters:

$$L_m = V_m t_m \tag{4}$$

$$a_m = V_m/t_m \tag{5}$$

The following dimensionless parameters are introduced: $V_m/\bar{V}_f$, $t_R/\bar{t}_f$, $t_m/\bar{t}_f$, a_m/a_g, $L_m/\bar{h}$, and V_m/V_{fm}, where a_g stands for acceleration with geyser initiation (cm/s^2) corresponding to geyser initiation gravity level g_i.

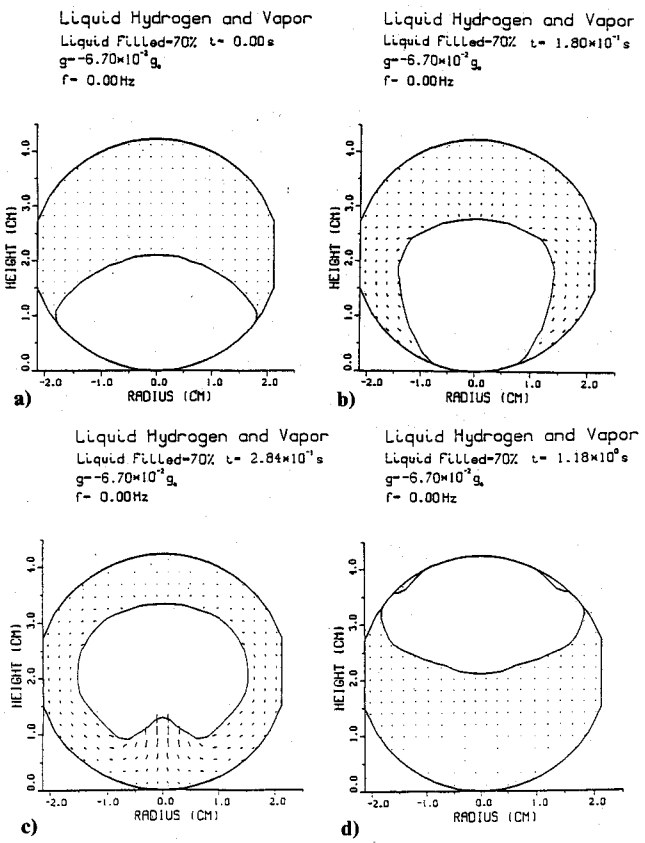

Fig. 5 Selected sequences of time evolution of fluid reorientation with liquid-filled level of 70%: a) initial profile; b) flow profile before the initiation of geyser; c) flow profile with geyser; and d) flow profile after the ending of geyser.

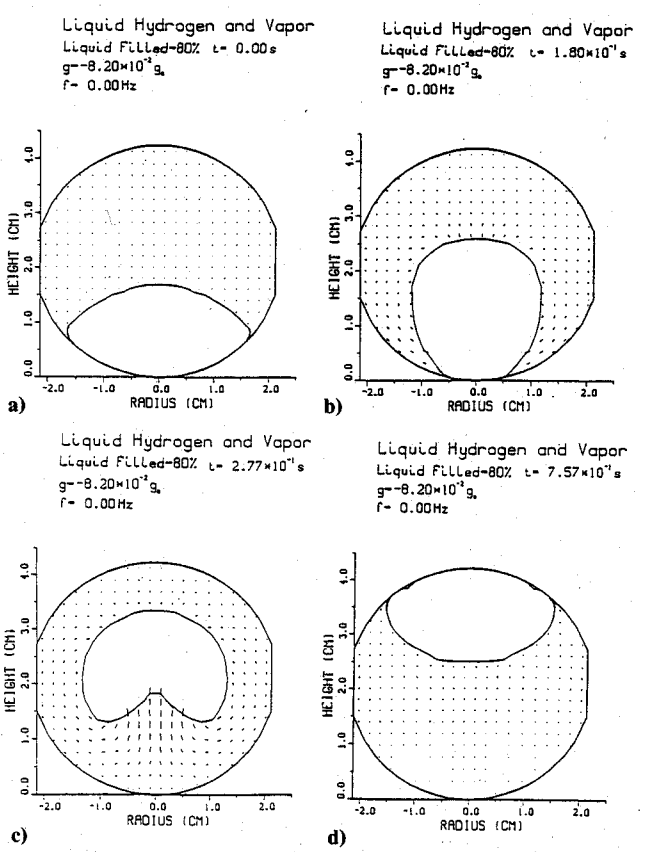

Fig. 6 Selected sequences of time evolution of fluid reorientation with liquid-filled levels of 80%: a) initial profile; b) flow profile before the initiation of geyser; c) flow profile with geyser; and d) flow profile after the ending of geyser.

Figures 7–9 show the variations of dimensionless parameters in terms of liquid-filled levels. Denominators of these six dimensionless parameters are either predetermined from the geometry of liquid-filled levels or can be deduced from the corresponding calculations associated with the geyser initiation gravity levels. Characteristics of these fairly constant values of dimensionless parameters can provide a good understanding of the physics of microgravity fluid behaviors.

Figure 7a shows the ratio of maximum flow velocity to average free-fall flow velocity $V_m/\bar{V}_f$ and its associated parameters of V_m and $\bar{V}_f$ in terms of liquid-filled levels. It shows that the ratio of $V_m/\bar{V}_f$ varies in the range of 4.3–4.9 in the entire liquid-filled levels while V_m and $\bar{V}_f$ vary from 62.0–73.6 cm/s (decreasing with increasing liquid-filled levels) and from 12.5–17.0 cm/s (also decreasing with increasing liquid-filled levels), respectively. As $\bar{V}_f$ can be predetermined from geyser initiation gravity level and average liquid height, shown in Eq. (1), one can make a prediction of maximum flow

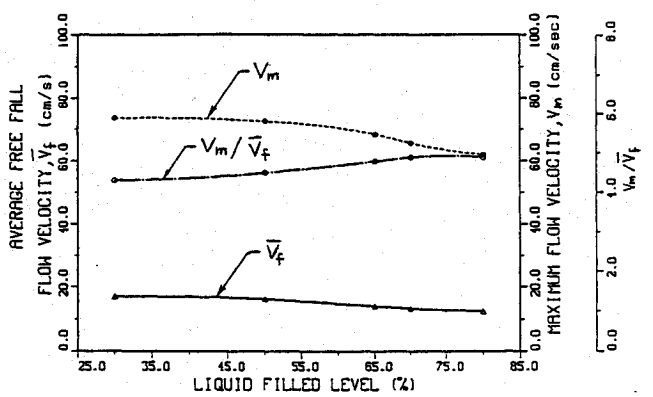

Fig. 7a Ratio of $V_m/\bar{V}_f$ and its associated parameters in terms of liquid-filled levels.

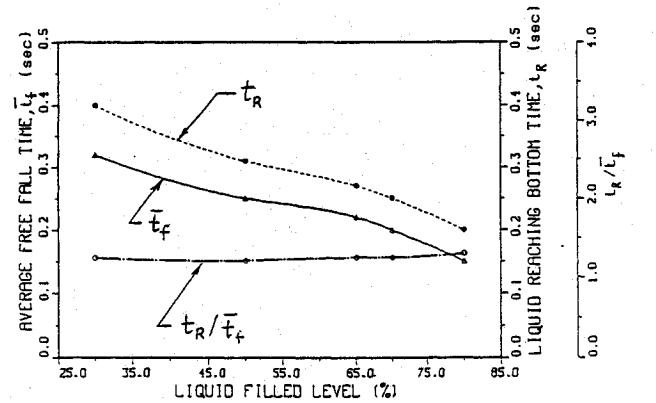

Fig. 7b Ratio of $t_R/\bar{t}_f$ and its associated parameters in terms of liquid-filled levels.

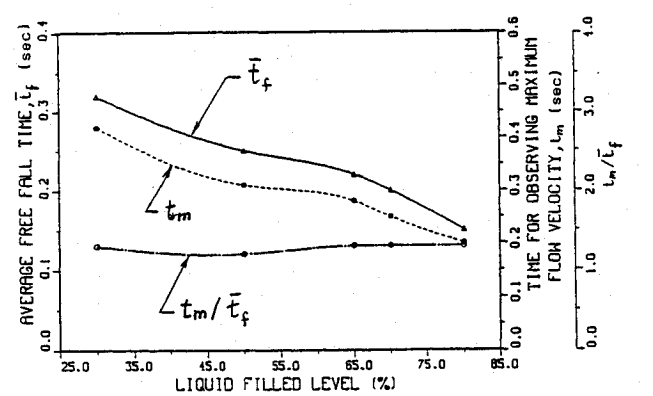

Fig. 8a Ratio of $t_m/\bar{t}_f$ and its associated parameters in terms of liquid-filled levels.

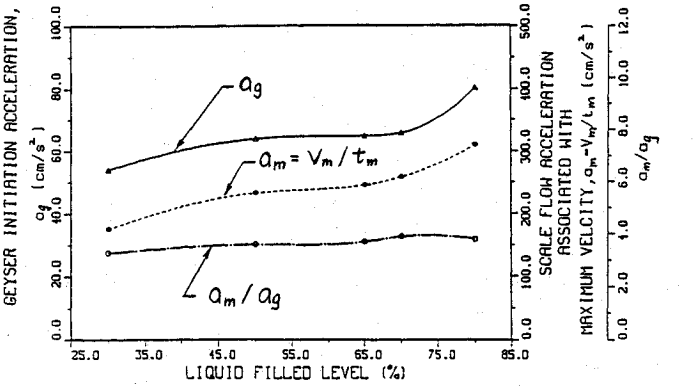

Fig. 8b Ratio of a_m/a_g and its associated parameters in terms of liquid-filled levels.

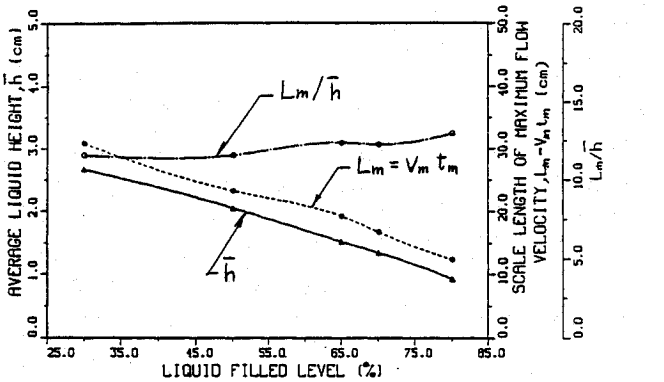

Fig. 9a Ratio of $L_m/\bar{h}$ and its associated parameters in terms of liquid-filled levels.

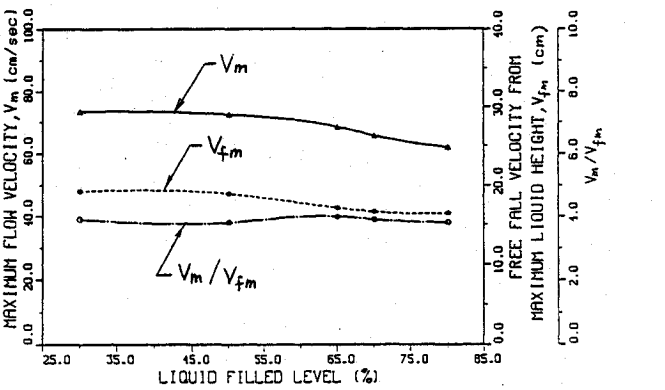

Fig. 9b Ratio of V_m/V_{fm} and its associated parameters in terms of liquid-filled levels.

velocity during the liquid reorientation for the various liquid-filled levels.

Figure 7b shows the ratio of time for liquid to reach tank bottom to average free-fall time $t_R/\bar{t}_f$ and its associated parameters of t_R and $\bar{t}_f$ in terms of liquid-filled levels. It shows that the ratio of $t_R/\bar{t}_f$ varies in the range of 1.21–1.30 in the entire liquid-filled levels while t_R and $\bar{t}_f$ vary from 0.20–0.40 s (decreasing with increasing liquid-filled levels) and from 0.15–0.32 s (also decreasing with increasing liquid-filled levels), respectively. As $\bar{t}_f$ can be predetermined from geyser initiation gravity level and average liquid height, shown in Eq. (2), one can predict the time required to reorient the liquid fluid from the original position to the bottom of the propellant tank for the various liquid-filled levels at the reverse gravity acceleration capable for the initiation of geyser.

Figure 8a shows the ratio of time needed for observing maximum flow velocity to average free-fall time $t_m/\bar{t}_f$ and its associated parameters of t_m and $\bar{t}_f$ in terms of liquid-filled

levels. It shows that the ratio of $t_m/\bar{t}_f$ varies in the range of 1.2–1.3 in the entire liquid-filled levels while t_m and $\bar{t}_f$ vary from 0.20–0.42 s (decreasing with increasing liquid-filled levels) and from 0.15–0.32 s (also decreasing with increasing liquid-filled levels), respectively. As we indicated in Fig. 7b, $\bar{t}_f$ can be predetermined, one can predict the time needed for observing maximum flow velocity for various liquid-filled levels at the reverse gravity acceleration capable for the initiation of geyser.

Figure 8b shows the ratio of scale flow acceleration associated with maximum velocity to acceleration with geyser initiation a_m/a_g and its associated parameters of a_m and a_g in terms of liquid-filled levels. It shows that the ratio of a_m/a_g varies in the range of 3.3–3.9 in the entire liquid-filled levels while a_m and a_g vary from 175–310 cm/s^2 (increasing with increasing liquid-filled levels) and from 53.9–80.4 cm/s^2 (also increasing with increasing liquid-filled levels), respectively. As a_g can be predetermined from geyser initiation gravity level, one can make a prediction of scale flow acceleration associated with maximum velocity, which is defined in Eq. (5), at the reverse gravity acceleration capable for the initiation of geyser.

Figure 9a shows the ratio of scale length of maximum flow velocity to average liquid height $L_m/\bar{h}$ and its associated parameters of L_m and $\bar{h}$ in terms of liquid-filled levels. It shows that the ratio of $L_m/\bar{h}$ varies in the range of 11.6–13.0 in the entire liquid-filled levels while L_m and $\bar{h}$ vary from 12.4–30.9 cm (decreasing with increasing liquid-filled levels) and from 0.93–2.67 cm (also decreasing with increasing liquid-filled levels), respectively. As $\bar{h}$ can be predetermined from the geometry of liquid-filled levels, one can make a prediction of scale length of maximum flow velocity, which is defined in Eq. (4), at the reverse gravity acceleration capable for the initiation of geyser.

Figure 9b shows the ratio of maximum flow velocity to free-fall velocity from maximum liquid height V_m/V_{fm} and its associated parameters of V_m and V_{fm} in terms of liquid-filled levels. It shows that the ratio of V_m/V_{fm} varies in the range of 3.8–4.0 in the entire liquid-filled levels while V_m and V_{fm} vary from 62.0–73.6 cm/s (decreasing with increasing liquid-filled levels) and from 16.4–19.2 cm/s (also decreasing with increasing liquid-filled levels), respectively. As V_{fm} can be predetermined from geyser initiation gravity level and maximum liquid height, shown in Eq. (3), one can make a prediction of maximum flow velocity at the reverse gravity acceleration capable for the initiation of geyser.

Six dimensionless parameters presented in this study show that the parameters hold fairly constant values through the entire ranges of liquid-filled levels during the course of liquid hydrogen reorientation activated by the reverse gravity acceleration with geyser initiation. As the denominators of these six dimensionless parameters are either predetermined from the geometry of liquid-filled levels or can be deduced from the corresponding calculations associated with the geyser initiation gravity levels, one can predict the flow parameters from these relations.

III. Discussion and Conclusions

The efficient management of subcritical cryogenic propellants is one of the key technology drivers for the on-orbit spacecraft. Cryogenic liquids are essential for the spacecraft as reactants, coolants, and propellants. The requirement to settle or to position liquid fuel over the outlet end of the spacecraft propellant tank prior to main engine restart poses a microgravity fluid behavior problem.

Flow profile simulations, in particular the time evolution of liquid-vapor interface during the course of fluid reorientation, for the various liquid-filled levels of 30, 50, 65, 70, and 80% are shown in Figs. 2–6. Table 1 and Figs. 7–9 show the characteristics of dimensionless flow parameters and their associated flowfields during the course of fluid reorientation with geyser initiation. Computer simulation of flowfields disclose the following results: 1) Geyser initiation gravity level is high for high liquid-filled level and vice versa. 2) Average liquid height is high for low liquid-filled level and vice versa. 3) Average free-fall flow velocity is high for low liquid-filled level and vice versa. 4) Maximum flow velocity is high for low liquid-filled level and vice versa. 5) Average free-fall time is longer for low liquid-filled level and vice versa. 6) Time required for liquid falling from original position to the bottom of the tank is longer for low liquid-filled level and vice versa. 7) Time needed for observing maximum flow velocity is longer for low liquid-filled level and vice versa. 8) Scale length of maximum flow velocity is longer for low liquid-filled level and vice versa. 9) Scale flow acceleration associated with maximum flow velocity is low for low liquid-filled level and vice versa. 10) Maximum liquid height is high for low liquid-filled level and vice versa. 11) Free-fall velocity from maximum liquid height is high for low liquid-filled level and vice versa.

Based on the computer simulation of flowfields during the course of fluid reorientation, six dimensionless parameters are presented in this study. It is shown, in Figs. 7–9, that these parameters hold fairly constant values through the entire ranges of liquid-filled levels during the course of fluid reorientation activated by the reverse gravity acceleration with geyser initiation. As the denominators of these dimensionless parameters are either predetermined from the geometry of liquid-filled levels or can be deduced from the corresponding calculations associated with the geyser initiation gravity levels, one can predict the values of these flow parameters from the relationship shown in Eqs. (1–5).

Any fluid capable of motion relative to the spacecraft will be subject to an acceleration relative to the mass center of the spacecraft that arises from the gravity gradient of the Earth.[21,22] In addition to the Earth's gravitational force, the interaction between the particle mass of fluids and the spacecraft mass due to gravity gradient accelerations (with container axis pointing toward the Earth, and variations of gravity gradient in radial and axial directions of container)[21] has also been taken into consideration in this microgravity fluid management study.

To conclude, we have demonstrated that the computer algorithm presented can be used to simulate fluid behavior in a microgravity environment, in particular the development of technology necessary for acquisition or positioning of liquid and vapor within a tank to enable liquid outflow or vapor venting through active liquid acquisition by the creation of a positive acceleration environment resulting from propulsive thrust. A better understanding of the full picture of flowfields during the course of fluid reorientation can provide better design techniques for handling and managing the cryogenic liquid propellants to be used in on-orbit spacecraft propulsion.

Acknowledgments

The authors appreciate the support received from NASA Headquarters through NASA Grant NAGW-812, and NASA Marshall Space Flight Center through NASA Contract NAS8-36955/Delivery Order No. 69.

References

[1]Anon., *Technology for Future NASA Missions: Civil Space Technology Initiative and Pathfinder,* NASA Office of Aeronautics and Space Technology, NASA CP-3016, 1988, pp. 568.

[2]Leslie, F. W., "Measurements of Rotating Bubble Shapes in a Low Gravity Environment," *Journal of Fluid Mechanics,* Vol. 161, No. 12, 1985, pp. 269–279.

[3]Hung, R. J., and Leslie, F. W., "Bubble Shape in a Liquid Filled Rotating Container Under Low Gravity," *Journal of Spacecraft and Rockets,* Vol. 25, No. 1, 1988, pp. 70–74.

[4]Hung, R. J., Tsao, Y. D., Hong, B. B., and Leslie, F. W., "Time Dependent Dynamical Behavior of Surface Tension on Rotating Fluids under Microgravity Environment," *Advances in Space Research,* Vol. 8, No. 12, 1988, pp. 205–213.

[5]Hung, R. J., Tsao, Y. D., Hong, B. B., and Leslie, F. W., "Bubble Behaviors in a Slowly Rotating Helium Dewar in Gravity Probe-B Spacecraft Experiment," *Journal of Spacecraft and Rockets,* Vol. 26,

No. 3, 1989, pp. 167–172.

[6]Hung, R. J., Tsao, Y. D., Hong, B. B., and Leslie, F. W., "Dynamical Behavior of Surface Tension on Rotating Fluids in Low and Microgravity Environments," *International Journal for Microgravity Research and Applications,* Vol. 11, No. 2, 1989, pp. 81–95.

[7]Hung, R. J., Tsao, Y. D., Hong, B. B., and Leslie F. W., "Axisymmetric Bubble Profiles in a Slowly Rotating Helium Dewar Under Low and Microgravity Environments," *Acta Astronautica,* Vol. 19, May 1989, pp. 411–426.

[8]Everitt, F., Parkinson, B., and Turneaure, J., "Stanford Relativity Gyroscope Experiment (NASA Gravity Probe-B)," *Proceedings of Society of Photo-Optical Instrumentation Engineers,* Vol. 619, Society of Photo-Optical Instrumentation Engineers, Bellingham, WA, 1986, pp. 1–165.

[9]Kamotani, Y., Prasad, A., and Ostrach, S., "Thermal Convection in an Enclosure Due to Vibrations Aboard a Spacecraft," *AIAA Journal,* Vol. 19, No. 4, 1981, pp. 511–516.

[10]Hung, R. J., Lee, C. C., and Shyu, K. L., "Reorientation of Rotating Fluid in Microgravity Environment with and without Gravity Jitters," *Journal of Spacecraft and Rockets,* Vol. 28, No. 1, 1991, pp. 71–78.

[11]Hung, R. J., Lee, C. C., and Leslie, F. W., "Effects of G-Jitters on the Stability of Rotating Bubble Under Microgravity Environment," *Acta Astronautica,* Vol. 21, No. 5, 1990, pp. 309–321.

[12]Hung, R. J., Lee, C. C., and Leslie, F. W., "Response of Gravity Level Fluctuations on the Gravity Probe-B Spacecraft Propellant System," *Journal of Propulsion and Power,* Vol. 7, No. 4, 1991, pp. 556–564.

[13]Hung, R. J., and Shyu, K. L., "Cryogenic Liquid Hydrogen Reorientation Activated by High Frequency Impulsive Reverse Gravity Acceleration of Geyser Initiation," *Microgravity Quarterly,* Vol. 1, No. 2, 1991, pp. 81–92.

[14]Hung, R. J., Lee, C. C., and Leslie, F. W., "Slosh Wave Excitation in a Partially Filled Rotating Tank Due to Gravity-Jitters in a Microgravity Environment," *Acta Astronautica,* Vol. 25, No. 8/9, 1991, pp. 523–551.

[15]Hung, R. J., and Shyu, K. L., "Space-Based Cryogenic Liquid Hydrogen Reorientation Activated by Low Frequency Impulsive Reverse Thruster of Geyser Initiation," *Acta Astronautica,* Vol. 25, No. 11, 1991, pp. 709–719.

[16]Harlow, F. H., and Welch, F. E., "Numerical Calculation of Time-Dependent Viscous Incompressible Flow of Fluid with Free Surface," *Physics of Fluids,* Vol. 8, No. 12, 1965, pp. 2182–2189.

[17]Spalding, D. B., "A Novel Finite-Difference Formulation for Differential Expressions Involving Both First and Second Derivatives," *International Journal of Numerical Methods in Engineering,* Vol. 4, No. 4, 1972, pp. 551–559.

[18]Patanker, S. V., *Numerical Heat Transfer and Fluid Flow,* Hemisphere-McGraw-Hill, New York, 1980, pp. 197.

[19]Patanker, S. V., and Spalding, S. D., "A Calculation Procedure for Heat, Mass and Momentum Transfer in Three Dimensional Parabolic Flows," *International Journal of Heat Mass Transfer,* Vol. 15, No. 6, 1972, pp. 1787-1805.

[20]Hung, R. J., and Shyu, K. L., "Slosh Wave Excitation Associated with High Frequency Impulsive Reverse Gravity Acceleration of Geyser Initiation," *Microgravity Quarterly,* Vol. 1, No. 3, 1991, pp. 125–133.

[21]Misner, C. W., Thorne, K. S., and Wheeler, J. A., *Gravitation,* W. H. Freeman, San Francisco, CA, 1973, pp. 1–1279.

[22]Forward, R. L., "Flattening Space-Time near the Earth," *Physical Review,* Series D, Vol. 26, No. 8, 1982, pp. 735–744.

Paul F. Mizera
Associate Editor